Negative Strategies

Numerical simulation of a vectored axisymmetric nozzle

Cite as: AIP Conference Proceedings **2293**, 200018 (2020); https://doi.org/10.1063/5.0026531
Published Online: 25 November 2020

Roberto Marsilio, Michele Ferlauto, and M. Hadi Hamedi-Estakhrsar

Numerical Simulation of a Vectored Axisymmetric Nozzle

Roberto Marsilio[1], Michele Ferlauto[1,a)] and M. Hadi Hamedi-Estakhrsar[2]

[1]*Department of Mechanical and Aerospace Engineering, Politecnico di Torino, Turin, Italy*

[2] *Department of Aerospace Engineering, K.N. Toosi University of Technology, Tehran, Iran*

[a)]Corresponding author: michele.ferlauto@polito.it

Abstract. A CFD based approach to the fully three-dimensional simulation of vectored nozzle is presented. The underlying technology used is based on an active flow control technique known as Fluidic Thrust-Vectoring. The flow governing equations are solved by using a finite volume discretization of the compressible Unsteady RANS equations. The numerical results obtained are compared with the experimental data found in the open literature.

INTRODUCTION

Thrust vectoring opened new perspective in the attitude control and maneuverability of aircraft. It allows unconventional maneuvers safely, even if the aircraft is in aerodynamic stalled conditions [1]. Actual multi-axis thrust vectoring technology is based on movable nozzles. Fluidic Thrust Vectoring (FTV) retains the advantages of mechanical thrust vectoring without the need of complex hardware with variable geometry [2]. FTV strategies follow the principle of flow manipulation to obtain a lateral force on a nozzle of fixed geometry. In general, the effect is obtained by injecting into the nozzle a secondary flow of bleed air. The injected fluid interacts with the exhaust flow into the fixed nozzle and, by breaking the symmetry, it generates wall pressure distributions that give rise to a side component of the thrust vector. The key point for the fluidic approach is the identification of a manipulation technique that can gradually modulate the symmetry-breaking effect within an acceptable range of deterioration of the nozzle performances [3]. Several manipulation strategies have been investigated in literature, such as, among others, the shock vector control, counterflows, throat shifting and the supersonic dual-throat nozzle concept [3]. Another very important aspect in practical applications of these technologies is that by using the same active flow control strategy one can overcome dangerous working conditions as for instance the instabilities that can arise in over-expanded or under-expanded nozzles. Experimental investigations of the efflux of the nozzle jet in calm air are feasible, but in-flight conditions are very difficult to be reproduced. Approaches based on the Computational Fluid Dynamics (CFD) became therefore the privileged mean of investigation for the evaluation of steady and unsteady vectored nozzle performances [4, 5]. An additional complication is that actual nozzles are generally axisymmetric and therefore deflected flow conditions become fully three-dimensional. The transient response of a typical nozzle system requires accurate 3D numerical simulations, dealing with natural and promoted flow separations, shock pattern formations, shock boundary layer interactions and more [6, 7].

In present work we start our road map towards a 3D framework for the simulation of the open and close loop simulation of the nozzle system, following the foot steps of the numerical tool already developed for the 2D case [5, 8–10]. As a reference nozzle we selected the Axisymmetric Dual-Throat Nozzle. For this nozzle concept, both experimental and numerical simulations are available in open literature [6, 7]. Moreover the ADTN has shown to have one of the best performances and, from the fluid dynamic perspective, it exhibit a very complex flow structure. In the next sections we describe the essential features of the numerical approach adopted and the validation of the steady performances of the ADTN configuration at several working conditions.

International Conference of Numerical Analysis and Applied Mathematics ICNAAM 2019
AIP Conf. Proc. 2293, 200018-1–200018-4; https://doi.org/10.1063/5.0026531
Published by AIP Publishing. 978-0-7354-4025-8/$30.00

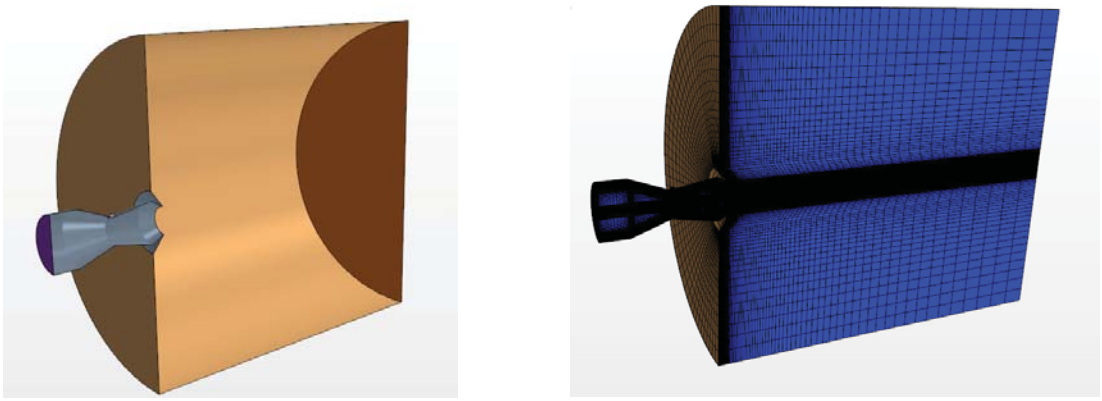

(a) (b)

FIGURE 1. Sketch of the axisymmetric dual-throat nozzle (a) and computational grid (b).

MATHEMATICAL MODEL

The fluid flow assumed as governed by the compressible Reynolds Averaged Navier-Stokes equations (RANS). The simulations have been carried out by using the CFD package StarCCM+, which is based on a finite-volume discretization of the flow governing equations. Several numerical investigations about nozzle flows have pointed out that turbulence modeling has a strong impact in the correct capture of the shock-boundary layer interactions [5, 11]. In particular, the use of wall-functions can lead to an incorrect prediction of the unsteady separation points. The full resolution of the boundary layers, without using wall-functions, even with a simpler one-equation model of turbulence must be preferred. Anyway, in many steady state simulations of the dual-throat nozzle [3, 7, 12] the RNG $k-\epsilon$ turbulence model with standard wall functions has been adopted. The results obtained were in good agreement with the related experimental data [6]. In the present study we selected the Spalart-Allmaras model without wall functions [13] for turbulence modeling. Briefly, the system of the governing equations can be described as follows

$$\frac{\partial \rho}{\partial t} + \frac{\partial}{\partial x_i}(\rho u_i) = 0 \tag{1}$$

$$\frac{\partial}{\partial t}(\rho u_i) + \frac{\partial}{\partial x_j}(\rho u_i u_j) = -\frac{\partial p}{\partial x_i} + \frac{\partial}{\partial x_j}\left[\mu\left(\frac{\partial u_i}{\partial x_j} + \frac{\partial u_j}{\partial x_i} - \frac{2}{3}\delta_{ij}\frac{\partial u_l}{\partial x_l}\right)\right] + \frac{\partial}{\partial x_j}(-\rho\overline{u_i' u_j'}) \tag{2}$$

$$\frac{\partial}{\partial t}(\rho E) + \frac{\partial}{\partial x_i}[u_i(\rho E + p)] = \frac{\partial}{\partial x_j}\left[\left(\kappa + \frac{C_p \mu_t}{P_{r_t}}\right)\frac{\partial T}{\partial x_j} + u_i(-\rho\overline{u_i' u_j'})\right] \tag{3}$$

which express mass, momentum and energy balance, respectively. As usual, ρ is density, p is pressure, μ is viscosity. Terms as u denote mean quantities, whereas u' is a fluctuating quantity. The terms $(-\overline{\rho u_i' u_j'})$ are the Reynolds-stress tensor. This set of equations require a turbulence closure model. A common starting point in modelling the Reynolds stresses is based on the Boussinesq assumption

$$(-\overline{\rho u_i' u_j'}) = \mu_t\left(\frac{\partial u_i}{\partial x_j} + \frac{\partial u_j}{\partial x_i}\right) - \frac{2}{3}\left(\rho K + \frac{\partial u_i}{\partial x_i}\delta_{ij}\right) \tag{4}$$

that relates the Reynolds stresses to the mean velocity gradients. The laminar viscosity μ is computed via the Sutherland's law. The reader is referred to Ref. [13] for the explanation of the S-A model. The Boundary Condition (BC) enforcement follows the guidelines of the characteristic based approach[14].

NUMERICAL RESULTS

The Axisymmetric Dual-Throat Nozzle (ADTN) concept is an axisymmetric convergent-divergent-convergent nozzle with two geometric minimum areas and a cavity formed by these areas. A sketch of the nozzle geometry in shown

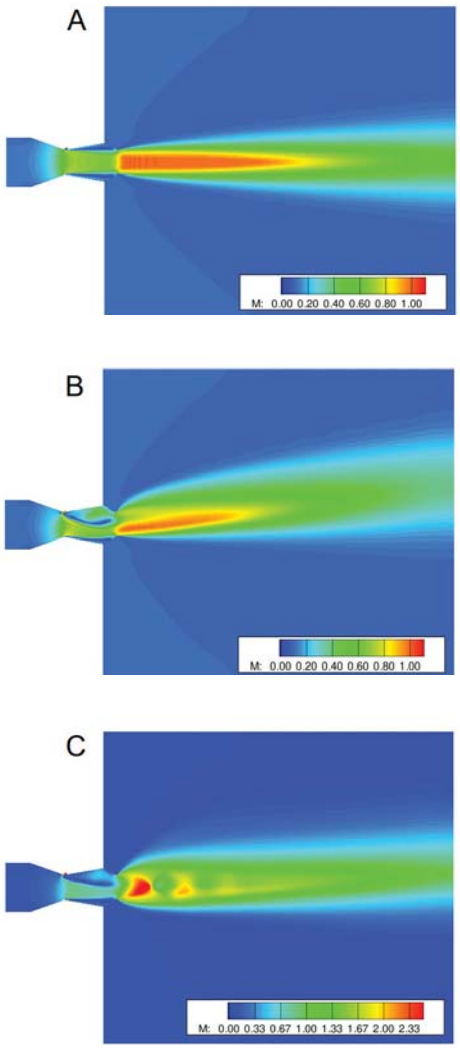

FIGURE 2. Mach number iso-contour maps of the flowfield inside the nozzle and in the discharge ambient. (A) NPR=1.89 without secondary jet; (B) NPR=1.89 $w_s = 3\%$; (C) NPR=3 $w_s = 3\%$. The cut-plane showed corresponds to the plane of symmetry of the nozzle.

in Figure 1a. The injection slot is located at the upstream minimum area. The details of nozzle geometry and of the injectors setup can be found in Ref. [6]. The case we considered here has equal minimum areas ($A_t/A_e = 1$) and a design nozzle pressure ratio NPR_d=1.89 . The injectors are placed radially and are equally spaced over an angle $\varphi_0 = 60^o$. The vectoring mechanism of the ADTN is similar to that occurring in the planar case. The one-side injection of secondary flow close to the first throat induces the flow separation at that station. The separated flow assesses itself in the recessed cavity and a cavity flow is formed. The flow and thrust deflection are therefore the result of the throat skewing effect, enhanced by the aerodynamic blockage generated by the vortical flow in the cavity region [5, 7]. With respect to the two-dimensional case, the vortex structure is supposed to be fully three-dimensional. induced separation and the generation of vortex flows in the cavity plays a major role in this jet-vectoring mechanism. As observed in many vortical flows [15] a weak forcing can lead the system to very different vortex pattern.

In the computational study performed we considered half of the nozzle domain, by introducing a plane of symmetry. This plane contains the axis of symmetry of the nozzle and splits the angle φ_0 in half, so that symmetry is preserved even when a flow deflection is present. The computational grid adopted has about 1 million of nodes and is represented in Figure1b. Grid stretching has been introduced in order to have $y^+ \simeq 1$ as required for turbulence modeling without wall functions. Two different nozzle pressure ratios (i.e. NPR=1.89 and NPR=3.0) have been considered,

in order to compare the results with the data available in Refs. [6, 7]. Some representations of the flowfields obtained are presented in Figure 2 in terms of Mach number iso-contour maps. The flowfield is represented on the symmetry plane. The ADTN case without secondary flow injection at NPR=1.89 is presented in Figure 2a. The flow symmetry and choked condition can be observed. At the same NPR=1.89 a secondary mass flow injection w_s with MFR=0.03 has been imposed, being MFR $= w_s/(w_p + w_s)$ the secondary mass flow ratio and w_p the primary nozzle mass flow. In this case, depicted in Figure 2b, the upward flow deflection is visible. The thrust deflection angle δ_p obtained is in close agreement with the experimental data ($\delta_p \simeq 15^o$. The flow structure is also confirmed. Finally, the case with NPR=3.0 and MFR=0.03 has been simulated. In this case the expansion in the external ambient is higher and also the maximum Mach number reached. The thrust vector angle is about $\delta_p = 13^o$. The computed flowfield is displayed in Figure 2c.

CONCLUSIONS

The proposed work illustrates an approach to the numerical simulation of active flow control in three dimensional nozzles. The analysis has been carried out on an axisymmetric configuration of the dual-throat nozzle, for which experimental and numerical data are available in the open literature [6, 7]. The numerical simulations have shown the ability of capturing the most relevant aspects of the complex flow pattern at different steady state working conditions. The simulation of the transient conditions is still needed for evaluating the accuracy on the prevision of the nozzle system dynamics. This is the first step of the extension to the three-dimensional case, that has higher relevance in actual applications, of a numerical framework for the thrust-vectoring and closed-loop nozzle flow control developed already in two dimensions. [5]

ACKNOWLEDGMENTS

Computational resources were provided by hpc@polito.it, a project of Academic Computing within the Department of Control and Computer Engineering at the Politecnico di Torino (http://www.hpc.polito.it). The financial support provided by Politecnico di Torino is gratefully acknowledged by the third author.

REFERENCES

[1] S. Asbury and F. Capone, Journal of Propulsion and Power **10**, 116–121 (1994).
[2] P. Yagle, D. *et al.*, ASME Journal of Engineering for Gas Turbines and Power **123**, 502–507 (2001).
[3] K. Deere, AIAA Paper 2003-3800, 21^{st} AIAA Appl. Aerodynamics Conf. (2003).
[4] M. Ferlauto and R. Marsilio, Advances in Aircraft and Spacecraft Science **3**, 367–378 (2016).
[5] M. Ferlauto and R. Marsilio, AIAA Journal **55**, 86–98 (2017).
[6] J. Flamm, *et al.* , AIAA paper 2007-5084, 43^{rd} AIAA Joint Prop. Conf. , (2007).
[7] K. Deere, *et al.* ,AIAA paper 2007-5085, 43^{rd} AIAA Joint Prop. Conf. (2006).
[8] E. Capello, A. *et al.*, Paper AIAA-2019-4311, 55^{th} AIAA Joint Prop. Conf. 1–10 (2019).
[9] M. Ferlauto and R. Marsilio, Advances in Aircraft and Spacecraft Science **5**, 349–362 (2018).
[10] M. Ferlauto and R. Marsilio, Paper AIAA-2019-4343, 55^{th} AIAA Joint Prop. Conf. 1–10 (2019).
[11] C. Tian and Y. Lu, Engineering Applications of Computational Fluid Mechanics **7**, 182–192 (2013).
[12] R. Gu, J. Xu, and S. Guo, ASME Journal of Engineering for Gas Turbines and Power **136**, 084501–1 (2014).
[13] P. Spalart, F. Johnson, and S. Allmaras, paper ICCFD7-1902, 7th Int. Conf. on Comp. Fluid Dyn., (2012).
[14] T. Poinsot and S. Lele, Journal of Computational Physics **101**, 104–129 (1992).
[15] A. Elcrat *et al.*, Fluid Dynamics Research **46**, p. 031407 (2014).